

Rapid Communications

Rapid Communications are intended for the accelerated publication of important new results and are therefore given priority treatment both in the editorial office and in production. A Rapid Communication in Physical Review B should be no longer than four printed pages and must be accompanied by an abstract. Page proofs are sent to authors.

Role of quantum fluctuations in the temperature dependence of intragap absorption in an MX chain complex

Noritaka Kuroda and Motoki Ito*

Institute for Materials Research, Tohoku University, Katahira 2-1-1, Aoba-ku, Sendai 980-77, Japan

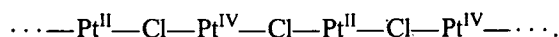
Masahiro Yamashita

College of General Education, Nagoya University, Chikusa-ku, Nagoya 464-01, Japan

(Received 13 June 1994)

We study the temperature dependence of persistent near-infrared absorption bands induced in single crystals of $[\text{Pt}(\text{en})_2][\text{Pt}(\text{en})_2\text{Cl}_2](\text{ClO}_4)_4$, where en=ethylenediamine, by irradiation with 488-nm light. If the temperature is changed between 10 and 200 K in dark after irradiation, these bands show significant changes in the spectral position, line shape, and intensity. The behaviors of the mean energy and second and third moments of the A band are interpreted consistently in terms of a quantum-fluctuation model of solitons bound by shallow, periodic potential wells.

Recent experiments of electron and nuclear paramagnetic resonance¹⁻⁵ have clarified that long-lived, mobile kink solitons possessing a spin of $S=\frac{1}{2}$ can be created by optical irradiation in an MX chain complex, $[\text{Pt}(\text{en})_2][\text{Pt}(\text{en})_2\text{Cl}_2](\text{ClO}_4)_4$, where en=ethylenediamine. (This substance is hereafter referred to as PtCl.) The unpaired spin is confined in the photoinduced domain wall which joins mutually antiphased charge-density-wave (CDW) states of Pt ions. The CDW of a single uniform chain can be denoted as follows:



The paramagnetic domain wall is self-localized into a valence structure of $\text{Pt}^{2.5} - \text{Cl}^- - \text{Pt}^{2.5}$: The unpaired spin spends 30–40 % of its time in the $3p_z\sigma$ orbital of the Cl^- ion at the center and spends most of the rest of its time in the $5d_{z^2}\sigma$ orbitals of the $\text{Pt}^{2.5}$ ions on both sides.⁴ Compared to the number of these solitons, very few paramagnetic polarons can be detected by electron paramagnetic resonance (EPR) as far as the crystal is irradiated at temperatures above about 40 K.

In PtCl, intense $\text{Pt}^{\text{II}} \rightarrow \text{Pt}^{\text{IV}}$ intervalence charge-transfer absorption occurs over a photon-energy region of 2.5–3.5 eV with its peak at 2.74 eV at 77 K.⁶ The above-mentioned solitons can be created through electron-transfer relaxation of photoexcited electron-hole pairs or of charge-transfer excitons.⁷ In concurrence with the appearance of the EPR signal, three intragap optical-absorption bands A, B, and B' are induced around 1.6, 2.0, and 2.1 eV, respectively.⁷⁻¹⁰ In this paper, we pay attention to the very broad and asymmetric line shape of the photoinduced bands, particularly the

A band. To explore the origin of this line shape, we perform a detailed study of its temperature dependence. The photoinduced absorption persists as long as the crystal is kept at a temperature below about 200 K. This property enables us, in contrast to the case of conjugated polymers, to observe the optically created states in a wide range of temperature. The results suggest that the line shape is dominated by the quantum fluctuation of solitons.

The temperature of the sample is regulated in a range of 10–200 K with a continuous-flow cryostat. The typical thickness of the sample is 80 μm . The sample is irradiated at 200 K by the 488-nm radiation of an Ar-ion laser, which is polarized *perpendicular* to the Pt—Cl chain axis b of the crystal. The laser is turned off once the sample is irradiated up to a given fluence. Afterward, the temperature dependence of the absorption spectrum is measured using a multichannel spectrometer equipped with a charge-coupled device (CCD) camera as the detector. A tungsten-halogen lamp is used as the light source. Light of wavelength longer than 520 nm is obtained with a glass filter and is polarized *parallel* to b by a Glan-Thompson prism. The shutter of the light source is synchronized with the shutter of the CCD camera. The typical exposure time chosen to take an absorption spectrum is 0.2 s. The intensity of the light source is set as low as possible in order to avoid the photoexcitation effect due to the light source.

Figure 1 shows the absorbance spectrum taken at 10 K after laser irradiation. In our samples, the inherent intragap absorption is very weak; its maximum absorption coefficient is $\sim 5 \text{ cm}^{-1}$,¹⁰ corresponding to an absorbance of ~ 0.04 in the present sample. Though the intervalence charge-transfer (CT) absorption is rather forbidden for the light with electric

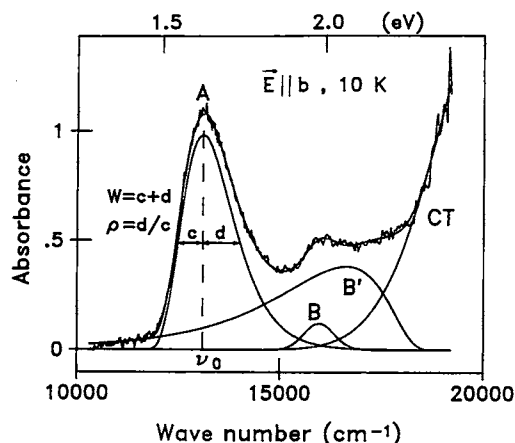


FIG. 1. Least-squares curve fit to the photoinduced absorption spectrum at 10 K. The line with a random noise is the experimental spectrum. The smooth line on the experimental spectrum is the result of the curve fit.

field \mathbf{E} polarized $\mathbf{E} \perp b$,¹¹ the intragap bands A , B , and B' are induced by the $\mathbf{E} \perp b$ laser. Furthermore, an intense photoluminescence due to the self-trapped CT exciton¹² can be observed during irradiation. It is certain, therefore, that the photoexcitation occurs nearly homogeneously throughout the sample.

It is apparent that the line shape of the A band is asymmetric, showing greater width on the higher-energy side. The spectrum is quite smooth, and there is no indication of the presence of subsidiary features between A and B bands. The log-normal function is known to be appropriate for expressing such an asymmetric spectrum. Therefore, to see the variation of the individual bands with temperature quantitatively, we decompose the observed spectrum by using the log-normal function for A and B' bands and Gaussian function for the tail of the CT band; the B band is much weaker than the A and B' bands and its asymmetry seems subtle, so that Gaussian is used for the B band. As shown in Fig. 1, the asymmetry is measured by the ratio $\rho = d/c$, where c and d are the distances of the half-maximum positions from the peak position ν_0 . Thus the half width is given by $W = c + d$. Let the maximum absorbance be A_0 . Then the log-normal absorbance is given as a function of frequency ν by¹³

$$A(\nu) = A_0 \exp \left[- \frac{\ln^2}{(\ln \rho)^2} \left\{ \ln \left(\frac{\nu - \nu_0}{W} \frac{\rho^2 - 1}{\rho} + 1 \right) \right\}^2 \right], \quad (1)$$

where

$$\nu \geq \nu_0 - \frac{W\rho}{\rho^2 - 1} \quad \text{for } \rho \geq 1.$$

Otherwise $A(\nu) = 0$. We may obtain a good least-squares fit to the whole spectrum, as shown in Fig. 1, by the iteration method at all temperatures examined. Actually, the B' band is spread farther toward higher energies than the result of this curve-fit analysis.¹⁰ Some extent of quantitative uncertainty remains, therefore, for the deduced parameters of the B' band and for the steepness of the tail of the CT band. Such

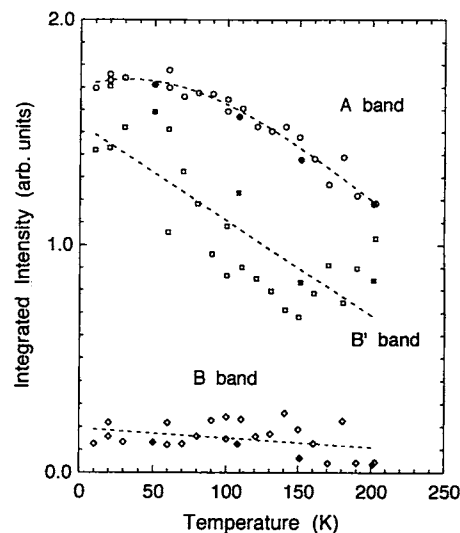


FIG. 2. Variation of the integrated intensities of the A (\circ, \bullet), B (\diamond, \blacklozenge), and B' (\square, \blacksquare) bands with temperature. Open and closed symbols denote the experimental values obtained on cooling and heating the sample, respectively, between 10 and 200 K. Dashed lines are drawn as guides.

uncertainty is irrelevant to other parameters, particularly for the A band, because below 2.0 eV the CT band absorption is negligibly weak.¹⁰

Figure 2 shows the integrated intensities, obtained for the three bands, as a function of temperature. The intensities of all the bands decrease with increasing temperature, though the data of the B and B' bands scatter largely. Note that these changes are reversible for temperature cycling within experimental errors. Evidently, the photoinduced states have a very long, practically infinite, lifetime under present experimental

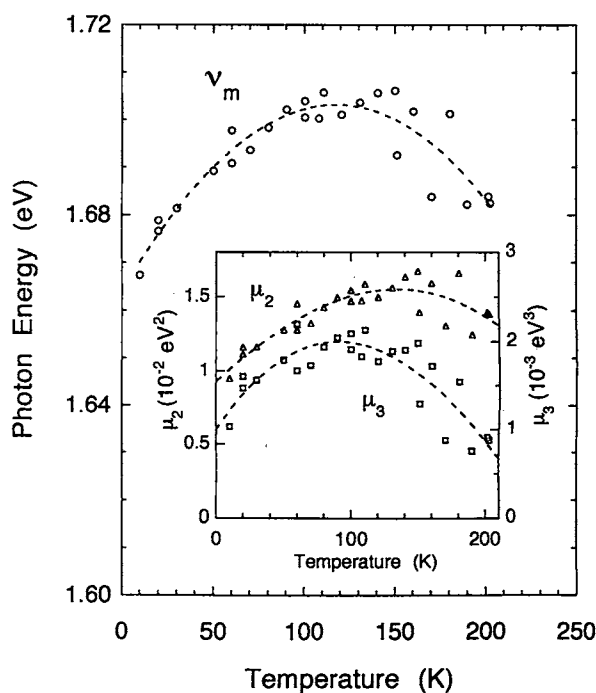


FIG. 3. Temperature dependence of ν_m (\circ), μ_2 (Δ), and μ_3 (\square) of the A band. Dashed lines are drawn as guides.

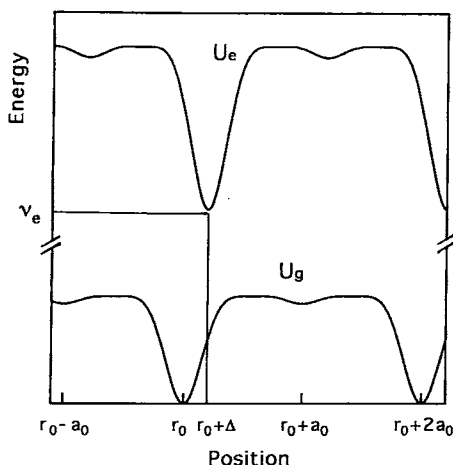


FIG. 4. A model of the ground- and excited-state potentials of the soliton as a function of the position in an MX chain. r_0 refers to an equilibrium position, a_0 to the nearest Pt-Pt distance in a chain, and Δ to the relative displacement of the potential minima.

conditions. In the following we look closely at the behavior of the A band.

The peak position ν_0 of the A band shifts from 1.62 to 1.65 eV on warming the crystal from 10 to 200 K. At the same time, the asymmetry parameter ρ decreases from 1.6 to 1.2, whereas the width W increases from 0.19 to 0.27 eV. As shown below, low-order moments of an asymmetric absorption band reflect the dynamical properties of a localized center. The log-normal function permits one to calculate those moments. The results of the first moment, i.e., the mean energy ν_m , second moment μ_2 , and third moment μ_3 , are shown in Fig. 3, where μ_2 and μ_3 are the means of $(\nu - \nu_m)^2$ and $(\nu - \nu_m)^3$, respectively, about the A band. We see that at 10 K both the damping factor $\sqrt{\mu_2}$ and the asymmetry factor $^3\sqrt{\mu_3}$ amount to 0.10 eV = 1200 K. In addition, not only μ_2 but also ν_m and μ_3 increase markedly with increasing temperature from 10 to about 100 K; the increase in ν_m , $\sqrt{\mu_2}$, and $^3\sqrt{\mu_3}$ amounts to 0.034 eV = 390 K, 0.028 eV = 320 K, and 0.026 eV = 300 K, respectively.

If the photoinduced state is disordered, the absorption band arising from it would be broadened. In fact, if the crystal is irradiated at a temperature below about 40 K, a strongly distorted EPR spectrum appears, showing that the photoinduced state is disordered. Accordingly, a cluster of phonon modes are observed in the photoinduced resonance Raman spectrum taken at 10–15 K.^{14,15} This disorder is, however, unstable above 40 K, so that the EPR spectrum resumes its original pattern if the crystal is annealed satisfactorily at a temperature higher than 40 K: The clearly defined superhyperfine structure^{1,2} indicates that the photoinduced state becomes quite homogeneous. It is for this reason that irradiation was made at temperatures 80–100 K in the previous EPR experiments.^{1–4} In the present work, irradiation is made at 200 K. As evidenced by the behavior of the intensity of the A band upon a temperature cycling between 10 and 200 K, the photoinduced state is thermalized well at all temperatures. In addition, the resonance Raman spectrum by the stretching mode of Cl^- ions proves a good homogeneity of the $\text{Pt}^{\text{II}}-\text{Cl}^--\text{Pt}^{\text{IV}}$ bond.¹⁶ In light of these facts, the large

values of μ_2 , μ_3 and their temperature coefficients are difficult to attribute to a static disorder effect. Furthermore, since the CT absorption peak shifts toward lower energies with increasing temperature,¹⁶ the behavior of ν_m at temperatures up to 100 K cannot be ascribed to the thermal change of the energy gap.

It has been recognized recently that a significant tail of the CT band, which is seen in Fig. 1, is caused by the zero-point vibration of Cl^- ions.¹⁶ In the present study, attributing the A band to solitons for the reasons mentioned at the beginning of this paper, we attempt to interpret our results in terms of the quantum fluctuation of those solitons. Figure 4 shows schematically the adiabatic potential energy as a function of the position in a chain. Note that the potential is not uniform.^{17,18} There are wells along a chain with a period of twice the nearest Pt-Pt distance a_0 . If the well is deep enough to trap a soliton, the trapped soliton would undergo a quantum vibration, of which the frequency depends on the effective soliton mass^{19,20} as well as the depth and width of the well. Since PtCl has a strong CDW, the effective mass m_s reaches to $(u_0/\xi)^2 M_{\text{Cl}} \sim 300m_0$, where ξ ($\sim a_0 = 5.4$ Å) is the size of the soliton, u_0 ($= 0.38$ Å) is the displacement of the Cl^- ions of the $\text{Pt}^{\text{II}}-\text{Cl}^--\text{Pt}^{\text{IV}}$ bond from the midpoint between Pt^{II} and Pt^{IV} , and M_{Cl} and m_0 are the masses of a Cl^- ion and a free electron, respectively. Though the value of m_s appears so large, it is yet much smaller than the proton mass. One may envisage that the large-amplitude zero-point motion plays a significant role in the optical responses.

To a first approximation one may express the potential wells of the ground and excited states, between which the electronic transition takes place, around an optimum position as

$$U_e = \nu_e + \frac{1}{2}\omega_e^2(r - \Delta)^2, \quad (2)$$

$$U_g = \frac{1}{2}\omega_g^2 r^2, \quad (3)$$

where the mass and Planck's constant are set to unity. The quantities ω_g and ω_e are the vibrational frequencies of a soliton in the ground and excited states, respectively, ν_e is the difference between the minima of the potentials, and Δ is the relative displacement of the minima along the MX chain axis r , which represents relaxation of the excited state caused by the electron-lattice coupling. Phenomenologically, this situation corresponds to the well-known configuration-coordinate model. According to Siano and Metzler,²¹ assuming an infinite series of the harmonic-oscillator levels,

$$\nu_m = \nu_e + \frac{1}{2}\omega_e^2\Delta^2 + \frac{(\omega_e^2 - \omega_g^2)}{4\omega_g} \coth\left(\frac{\omega_g}{2kT}\right), \quad (4)$$

$$\mu_2 = \frac{\omega_e^4\Delta^2}{2\omega_g} \coth\left(\frac{\omega_g}{2kT}\right) + \frac{(\omega_e^2 - \omega_g^2)^2}{8\omega_g^2} \coth^2\left(\frac{\omega_g}{2kT}\right), \quad (5)$$

$$\begin{aligned} \mu_3 = & \frac{3\omega_e^4\Delta^2(\omega_e^2 - \omega_g^2)}{4\omega_g^2} \coth^2\left(\frac{\omega_g}{2kT}\right) \\ & + \frac{(\omega_e^2 - \omega_g^2)^3}{8\omega_g^3} \coth^3\left(\frac{\omega_g}{2kT}\right), \end{aligned} \quad (6)$$

where k is the Boltzmann constant and T is temperature.

It is apparent from these formulas that the crucial factor for determining the values of ν_m and μ_3 is the magnitude of ω_e relative to ω_g . To see this aspect quantitatively, let us look at the experimental results at temperatures in a range of 10–60 K, where the solitons fall mostly into the zero-point level. The fact that ν_m has a positive temperature coefficient implies $\omega_e > \omega_g$, though the monotonous increase in ν_m suggests that the form $\coth\{\omega_g/2k(T+T^*)\}$, where $T^* \sim \omega_g/2k$,²² is rather rational than the form $\coth(\omega_g/2kT)$. Equation (6) claims further that if $\omega_e > \omega_g$, both the sign and temperature coefficient of μ_3 , as well as the temperature coefficient of μ_2 , should be positive. Our experimental results clearly justify this claim, proving that the configuration-coordinate model applies to the present case well. Substituting the experimental values of ν_m , μ_2 , and μ_3 into Eqs. (4), (5), and (6), respectively, we obtain $\omega_g = 0.02 \pm 0.01$ eV, $\omega_e/\omega_g = 3 \pm 1$, $\omega_e^2 \Delta^2/2 = 0.08 \pm 0.02$ eV, and $\nu_e = 1.58 \pm 0.01$ eV. The value of ω_g is comparable to the local-mode frequency of Cl^- ions.²³ The point of the present experimental result is that the asymmetry as well as the width is quite large compared to the lattice temperature. It turns out that μ_3 is dominated by the first term of Eq. (6). Namely, a large asymmetry arises from cooperation of a large value of Δ and a positive value of $\omega_e - \omega_g$.

We note from Fig. 3 that all the quantities ν_m , μ_2 , and μ_3 reach maximum around 100–150 K, and then decrease with increasing temperature: In particular, μ_3 decreases as it vanishes around 250 K. Simple thermal broadening effect cannot explain this phenomenon. It is worth here reminding

that, if a soliton is unbound, the absorption band should be ordinarily narrow as predicted by many theories;^{22–24} moreover ν_m must follow half the energy gap upon a change in temperature,¹⁹ that is, ν_m must decrease as temperature increases. Hence, within the framework of our model, it is natural to interpret the experimental results in the following way: The potential well of the ground state is so shallow that only a few vibrational levels are formed, and therefore above about 100 K solitons spend an appreciable time at unbound positions (see Fig. 4) as a result of thermal release from the well. Indeed, the activation energy for the translational motion of spin solitons is known to be 11–13 meV = 130–150 K,^{1,5} being in good agreement with the temperatures where ν_m , μ_2 , and μ_3 reach the maximum. Presumably, the pronounced temperature dependence of the absorption intensity (see Fig. 2) is related closely to this unique phenomenon.

In conclusion, we have found that the near-infrared absorption bands photoinduced in $[\text{Pt}(\text{en})_2][\text{Pt}(\text{en})_2\text{Cl}_2](\text{ClO}_4)_4$ exhibit pronounced variation of the energy, line shape, and intensity with temperature. The behaviors of the mean energy and second and third moments of the A band are interpreted consistently in terms of a simple configuration-coordinate model which takes account of the quantum vibration of solitons bound loosely by shallow and periodic potential wells. This property will be common to solitons and polarons in many MX chain complexes.

The authors acknowledge Dr. M. Sakai for valuable advice in the course of crystal growth.

*Present address: Kyocera Co., Yohkaich 527, Japan.

¹N. Kuroda, M. Sakai, M. Suezawa, Y. Nishina, and K. Sumino, *J. Phys. Soc. Jpn.* **59**, 3049 (1990).

²M. Sakai, N. Kuroda, M. Suezawa, Y. Nishina, K. Sumino, and M. Yamashita, *J. Phys. Soc. Jpn.* **61**, 1326 (1992).

³N. Kuroda, M. Sakai, M. Suezawa, Y. Nishina, K. Sumino, and M. Yamashita, *Mol. Cryst. Liq. Cryst.* **216**, 169 (1992).

⁴N. Kuroda, M. Ito, Y. Nishina, A. Kawamori, Y. Kodera, and T. Matsukawa, *Phys. Rev. B* **48**, 4245 (1993).

⁵R. Ikeda, A. Ghosh, L. S. Prabhuramirashi, D. Nakamura, and M. Yamashita, *Mol. Cryst. Liq. Cryst.* **216**, 181 (1992).

⁶Y. Wada and M. Yamashita, *Phys. Rev. B* **42**, 7398 (1990).

⁷M. Sakai, N. Kuroda, and Y. Nishina, *Phys. Rev. B* **40**, 3066 (1989).

⁸N. Kuroda, M. Sakai, Y. Nishina, M. Tanaka, and S. Kurita, *Phys. Rev. Lett.* **58**, 2122 (1987).

⁹S. Kurita, M. Haruki, and K. Miyagawa, *J. Phys. Soc. Jpn.* **57**, 1789 (1988).

¹⁰N. Kuroda, M. Ito, Y. Nishina, and M. Yamashita, *J. Phys. Soc. Jpn.* **62**, 2237 (1993).

¹¹N. Tanaka, S. Kurita, T. Kojima, and Y. Yamada, *Chem. Phys.* **91**, 257 (1984).

¹²H. Tanino, W. W. Ruhle, and K. Takahashi, *Phys. Rev. B* **38**, 12 716 (1988).

¹³D. E. Metzler, C. M. Harris, R. J. Johnson, and J. A. Thomson, *Biochem.* **12**, 5377 (1973).

¹⁴S. C. Hockett, R. J. Donohoe, L. A. Worl, A. D. Bulou, C. J. Burns, J. R. Laia, D. Carrol, and B. I. Swanson, *Chem. Mater.* **3**, 123 (1992).

¹⁵S. P. Love, L. A. Worl, R. J. Donohoe, S. C. Hockett, S. R. Johnson, and B. I. Swanson, *Synth. Met.* **55–57**, 3456 (1993).

¹⁶F. H. Long, S. P. Love, and B. I. Swanson, *Phys. Rev. Lett.* **71**, 762 (1993).

¹⁷N. Kuroda, M. Kataoka, and Y. Nishina, *Phys. Rev. B* **44**, 13 260 (1991).

¹⁸M. Suzuki and K. Nasu, *Phys. Rev. B* **45**, 1605 (1992).

¹⁹W. P. Su, in *Handbook of Conducting Polymers*, edited by T. K. Scothorn (Dekker, New York, 1986), Vol. 2, pp. 757–794.

²⁰Y. Onodera, *J. Phys. Soc. Jpn.* **56**, 250 (1987).

²¹D. B. Siano and D. E. Metzler, *J. Chem. Phys.* **51**, 1856 (1969).

²²K. Iwano and K. Nasu, *J. Phys. Soc. Jpn.* **61**, 1380 (1992).

²³I. Batistic, X. Z. Huang, A. R. Bishop, and A. Saxena, *Phys. Rev. B* **48**, 6065 (1993).

²⁴J. Gammel, A. Saxena, I. Batistic, and A. R. Bishop, *Phys. Rev. B* **45**, 6408 (1992); S. M. Milbrodt, J. Gammel, A. R. Bishop, and E. Y. Loh, *ibid.* **45**, 6435 (1992).